Many-body effects in the paramagnetic and antiferromagnetic states of the (111) silicon face

A. Muñoz, F. Flores, and C. Tejedor
Departamento de Física del Estado Sólido, Universidad Autónoma, Cantoblanco, 28049 Madrid, Spain

E. Louis
Departamento de Física, Facultad de Ciencias, Universidad de Alicante, Apartado Postal 99, 03080 Alicante, Spain and Endasa, Centro de Investigación y Desarrollo, Apartado Postal 25, 03080 Alicante, Spain

(Received 20 May 1985)

The electron density of surface states has been calculated for both the paramagnetic and the antiferromagnetic states of Si(111). Many-body effects associated with correlation and electron-phonon coupling are included. Our results have been obtained by using a self-consistent tight-binding approach, a Bethe-lattice method, and Green-function techniques. The paramagnetic phase shows a very narrow Kondo-like peak at the Fermi level E_F, two satellites at $E_F \pm 0.2$ eV, and two broader peaks at $E_F \pm 0.8$ eV. The antiferromagnetic phase shows two peaks at $E_F \pm 0.8$ eV and two others at $E_F \pm 0.4$ eV. In this case the energy gap of 0.6 eV due to correlation effects is reduced by electron-phonon coupling up to 0.25 eV.

I. INTRODUCTION

Despite the great deal of work on covalent surfaces, these systems continue to be a challenge to both theoretical and experimental researchers. Si(111) surfaces present two types of reconstruction; the (2×1) surface is obtained by cleavage, and the (7×7) reconstruction appears under annealing and remains stable when the temperature is lowered; an unreconstructed surface seems to have been obtained only by appropriate methods.[1,2] Many different models have been proposed for the two reconstructions. The π-bonded chain model,[3] modified by a buckling of the surface atoms for the (2×1) reconstruction, appears to be the only model consistent with recent ion-backscattering[4] and optical experiments;[5,6] however, low-energy electron-diffraction (LEED) results[7] only show a moderate agreement with the results given by Pandey's model, while photoemission experiments[8,9] for the surface bands of this (2×1) surface show some discrepancies with theoretical calculations.[10]

For the Si(111)-(7×7) reconstructed surface many different models have been proposed;[11–13] ion-backscattering experiments tend to favor Himpsel's[11] and McRae's[12] models, but there is no definitive explanation for this reconstruction. Recent experimental[14,15] evidence for the Si(111)-(7×7) surface suggests that correlation effects and electron-phonon coupling may play a major role in the surface properties associated with the dangling-bond surface states. Preliminary theoretical results have shown that, indeed, this is so for a metal-like surface:[16] This is expected to be the case for a Si(111)-(7×7) surface which seems to have an odd number of dangling bonds.

These results suggest that many-body effects may also be important for the Si(111)-(2×1) surface; these effects may be the source of the discrepancies commented on above for photoemission experiments. Prompted by these considerations and guided by previous theoretical work in two-dimensional systems,[17,18] we have started to analyze the surface of three-dimensional Si crystals by including correlation and electron-phonon interactions in the dangling-bond surface states.

In this paper, we present theoretical results for the paramagnetic and antiferromagnetic states of the Si(111) surface. Independently of the intrinsic interest that these ideal surfaces can have,[1,2] we think that this theoretical analysis may throw light on the importance of correlation and electron-phonon effects on the properties of covalent surface states. A similar analysis is under progress in our laboratory for the π-bond model of reconstructed surfaces.

II. THE MODEL

In this paper, we describe the electron band structure for Si by means of the Weaire-Thorpe Hamiltonian:[19] We introduce sp^3 hybrids for each atom and nearest-neighbor interaction in the crystal. Since correlation effects for the bulk crystal have been shown to be small,[20] we only introduce in our model an intrasite Coulomb interaction for the dangling bonds. Accordingly, the electronic part of our Hamiltonian is the following:

$$\hat{H}_{\rm el}=\sum_{d,\sigma}(E_s-\tfrac{1}{2}U)n_{d,\sigma}+\sum_{\substack{s,\sigma,\\ u\,(\neq d)}}E_s n^u_{s,\sigma}+\sum_{\substack{i\,(\neq s,d),\\ u,\sigma}}E_b n^u_{i,\sigma}+\sum_{\substack{i,\\ u\,(\neq v)}}t_0 c^{u\dagger}_{i,\sigma}c^{v}_{i,\sigma}+\sum_{\substack{u,v\\ (i\neq j)}}t_{ij}c^{u\dagger}_{i,\sigma}c^{v}_{j,\sigma}+\sum_d U n_{d\uparrow}n_{d\downarrow}\,, \tag{1}$$

where $n_{d,\sigma}$, $n^u_{s,\sigma}$, and $n^u_{i,\sigma}$ are the dangling bonds, the other surface layer orbitals, and the bulk orbital occupation number operators, respectively; t_0 is the hopping integral inside each atom, while t_{ij} defines the hopping integrals between orbitals u and v of nearest neighbors i and j. In Hamiltonian (1), the surface level E_s is adjusted to get charge neutrality in the last layer. Note that a Hartree solution to Hamiltonian (1) is equivalent to substituting $E_s - U/2$ for E_s and to eliminating $Un_{d\uparrow}n_{d\downarrow}$ from Eq. (1).

On the other hand, we introduce the electron-phonon interaction in the following way. Since we are interested mostly in the effect of the phonons on the surface states, we only introduce the phonons associated with the last atomic layer. Note that surface states are mostly localized in the last atomic layer, and that the electrons are more strongly coupled with the optical phonons of the crystal. In a first approximation, the electron-phonon coupling for the optical phonons of a covalent semiconductor is a localized interaction between the electrons of an atom and its local vibration.[21] This suggests the introduction of an Einstein model for phonons and the following electron-phonon interaction:

$$H_{e\text{-ph}} = \sum_i \omega_0 (b_s^\dagger b_s + \tfrac{1}{2}) + g^{1/2}\omega_0 \sum_s (N_s - 1)(b_s^\dagger + b_s) \, . \quad (2)$$

In this equation, $b_s^\dagger$ and b_s are the boson operators associated with the phonons of frequency ω_0 for the surface atom s. In Hamiltonian (2), the local phonons are coupled to the electrons filling the orbitals of the same surface atom s. In principle, the phonon is coupled to all the electrons of the atom; however, the interaction with the electrons filling the valence band is small and of no interest in our case. We are rather interested in the electrons filling the surface states. Accordingly, in Eq. (2), *N_s is the occupation number associated with the dangling-bond occupancy;* note that the mean occupancy of a dangling bond is 1, in such a way that the factor $N_s - 1$ of Eq. (2) is related to the fluctuation of the electronic charge around that mean value.

As regards the electron-phonon coupling, measured by the constant g in Hamiltonian (2), we have taken the value obtained in a self-consistent calculation for the optical phonons[20] of Si, renormalized by the effective charge filling the surface states in the surface layer. This value corresponds to the crystal bulk constant, multiplied by a filling factor of ~ 0.7 (see below); in principle, for the surface this coupling constant would have to be screened also by the surface-state electrons. However, due to the electron correlation effects associated with the strong intrasite Coulomb interaction for the dangling-bond orbitals, the local density of states near the Fermi level is low[17] (see below), and the value of the coupling constant g at the surface can be assumed to be unscreened.

Hamiltonians (1) and (2) define the model we are going to discuss. We analyze these Hamiltonians in two steps: (i) In Sec. III we discuss correlation effects on the electronic states of the paramagnetic and antiferromagnetic Si(111) surface; (ii) in Sec. IV we consider the electron-phonon coupling effects.

III. CORRELATION EFFECTS

A. Method of solution

In this section we discuss the procedure we have followed to analyze the antiferromagnetic Si(111)-(2×1) face. The paramagnetic Si(111)-(1×1) face has been discussed elsewhere, and the reader is referred to Ref. 22.

Figure 1 shows a top view of the Si(111)-(2×1) face, with two different rows of atoms, α and β, having different densities of states for a given spin. We look for the antiferromagnetic solution by introducing Green-function techniques and appropriate self-energies. Thus, Hamiltonian (1) can be substituted for

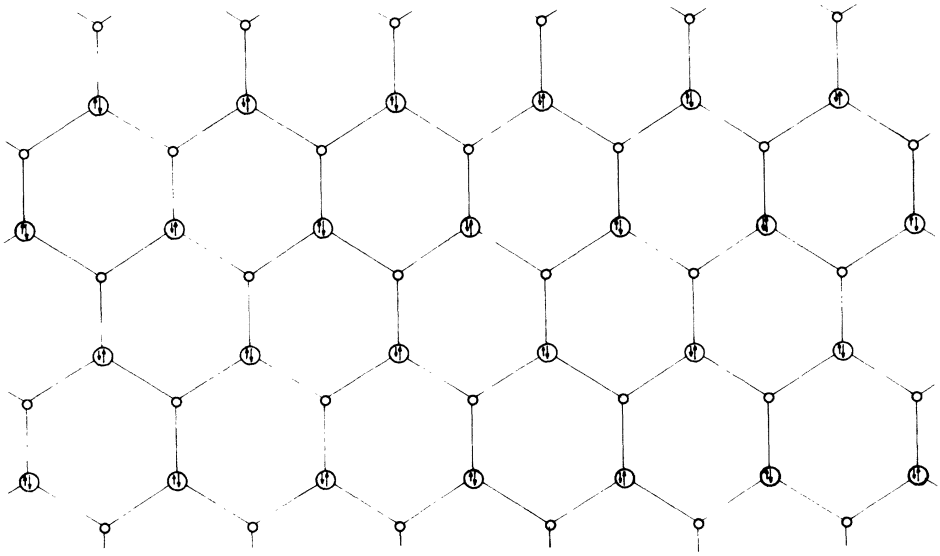

FIG. 1. Top view of the antiferromagnetic Si(111)-(2×1) face.

$$H_e=\sum_{d,\sigma}[E_s+U\delta\langle n_{d,\bar{\sigma}}^{(\alpha)}\rangle+\Sigma_{d,\sigma}^{(\alpha)}(\omega)]n_{d,\sigma}^{(\alpha)}+\sum_{d,\sigma}[E_s+U\,\delta\langle n_{d,\bar{\sigma}}^{(\beta)}\rangle+\Sigma_{d,\sigma}^{(\beta)}(\omega)]n_{d,\sigma}^{(\beta)}$$
$$+\sum_{\substack{s,\sigma,\\ u\,(\neq d)}}E_s n_{s,\sigma}^{u}+\sum_{\substack{i\,(\neq s,d),\\ u,\sigma}}E_b n_{i,\sigma}^{u}+\sum_{\substack{i,\\ u,v\\ (u\neq v)}}t_0 c_{i,\sigma}^{u\dagger}c_{i,\sigma}^{v}+\sum_{\substack{i,j,\\ u,v\\ (i\neq j)}}t_{ij}c_{i,\sigma}^{u\dagger}c_{j,\sigma}^{v}\ , \tag{3}$$

where the term $Un_{d\uparrow}n_{d\downarrow}$ of Hamiltonian (1) has been substituted for $U\langle n_{d,\sigma}^{(\alpha)}\rangle$, $U\langle n_{d,\sigma}^{(\beta)}\rangle$, $\Sigma_{d,\sigma}^{(\alpha)}(\omega)$, and $\Sigma_{d,\sigma}^{(\beta)}(\omega)$, with $\langle n_{d,\sigma}\rangle=\int_{-\infty}^{E_F}n_{d,\sigma}(\omega)d\omega$. In Eq. (3), E_s is the mean level of the surface layer, adjusted to give charge neutrality in the last layer. Hamiltonian (3) can be used to calculate the electron density of states *if* the self-energies $\Sigma_{d,\sigma}^{(\alpha)}$ and $\Sigma_{d,\sigma}^{(\beta)}$ associated with the dangling bonds of the two kind of atoms α and β at the surface are known. Self-energies are calculated by following the procedure discussed in Ref. 17; to this end, we introduce the following effective Hamiltonian:

$$\hat{H}_{\rm eff}=\sum_{d,\sigma}E_{{\rm eff},\sigma}^{(\alpha)}n_{d,\sigma}^{(\alpha)}+\sum_{d,\sigma}E_{{\rm eff},\sigma}^{(\beta)}n_{d,\sigma}^{(\beta)}+\sum_{\substack{\sigma,\\ u\,(\neq d)}}E_s n_{s,\sigma}^{u}+\sum_{\substack{i\,(\neq s,d),\\ u,\sigma}}E_b n_{i,\sigma}^{u}+\sum_{\substack{i,\\ u,v\\ (u\neq v)}}t_0 c_{i,\sigma}^{u\dagger}c_{i,\sigma}^{v}+\sum_{\substack{i,j,\\ u,v\\ (i\neq j)}}t_{ij}c_{i,\sigma}^{u\dagger}c_{j,\sigma}^{v}\ , \tag{4}$$

and calculate the effective one-electron density of states $n_{{\rm eff},d,\sigma}^{(i)}(\omega)$ for the dangling bond d. Then we define the following second-order self-energies:

$$(\Sigma_{d,\sigma}^{(i)})^{(2)}(\omega)=U^2\int_{-\infty}^{E_F}d\omega_2\int_{E_F}^{\infty}d\omega_3\int_{E_F}^{\infty}d\omega_4\frac{n_{{\rm eff},d,\sigma}^{(i)}(\omega_2)n_{{\rm eff},d,\sigma}^{(i)}(\omega_3)n_{{\rm eff},d,\sigma}^{(i)}(\omega_4)}{\omega+\omega_2-\omega_3-\omega_4+i\eta}$$
$$+U^2\int_{E_F}^{\infty}d\omega_2\int_{-\infty}^{E_F}d\omega_3\int_{-\infty}^{E_F}d\omega_4\frac{n_{{\rm eff},d,\sigma}^{(i)}(\omega_2)n_{{\rm eff},d,\sigma}^{(i)}(\omega_3)n_{{\rm eff},d,\sigma}^{(i)}(\omega_4)}{\omega+\omega_2-\omega_3-\omega_4+i\eta}\ , \tag{5}$$

where $i=\alpha,\beta$, and we introduce the following self-energies to all orders of U:

$$\Sigma_{d,\sigma}^{(i)}(\omega)=(\Sigma_{d,\sigma}^{(i)})^{(2)}(\omega)\Big/\left[1-\frac{E_s-\frac{1}{2}U+(1-\langle n_{d,\sigma}^{i}\rangle)U-E_{{\rm eff},\sigma}^{(i)}}{\langle n_{d,\sigma}^{i}\rangle(1-\langle n_{d,\sigma}^{i}\rangle)U^2}(\Sigma_{d,\sigma}^{(i)})^{(2)}(\omega)\right]\ , \tag{6}$$

for the dangling-bond surface states.

Effective levels $E_{{\rm eff},\sigma}^{(i)}$ are determined by imposing self-consistency for the dangling-bond charges $\langle n_\sigma^i\rangle$ as calculated from Hamiltonians (3) and (4). Let us comment at this point that the symmetry of the problem yields the following identities:

$$\langle n_\sigma^\alpha\rangle=\langle n_\sigma^\beta\rangle\ , \tag{7a}$$

$$E_{{\rm eff},\sigma}^{\alpha}=E_{{\rm eff},\sigma}\ , \tag{7b}$$

and

$$\Sigma_{d,\sigma}^{(\alpha)}(\omega)=\Sigma_{d,\sigma}^{(\beta)}(\omega)\ . \tag{7c}$$

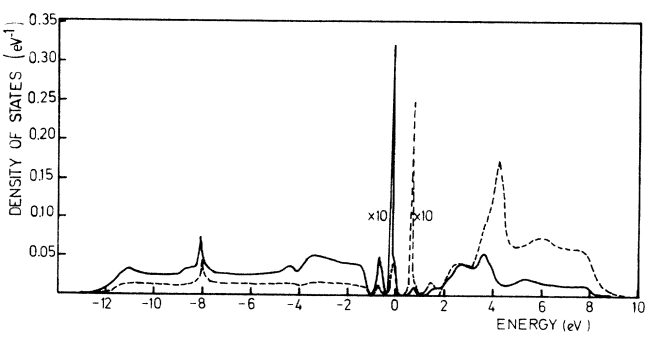

FIG. 2. Local density of states for the dangling bond of the Si(111)-(2×1) face, with $U=5.5$ eV. Solid line: spin up. Dashed line: spin down.

The final point to discuss in this section is the procedure we have followed to calculate the density of states in the surface layer. In this paper we have used the Bethe-lattice method[23] adapted to the (2×1) surface. In this method, Dyson's equation, $(\omega-\hat{H})\hat{G}=\mathbf{1}$, is projected on the orbitals of atoms n and 0 (see Fig. 1). This yields the following equations (see Ref. 23):

$$\begin{aligned}
&(\underline{1}E-\underline{V}_\alpha^\sigma)\underline{G}_{0,0,\sigma}=\underline{1}+\underline{V}_3\underline{G}_{1,0,\sigma}+\underline{V}_2\underline{G}_{3,0,\sigma}+\underline{V}_4\underline{G}_{5,0,\sigma}\ ,\\
&(\underline{1}E-\underline{V}_b-\underline{U}_1\underline{T}_1)\underline{G}_{1,0,\sigma}=\underline{V}_3\underline{G}_{0,0,\sigma}+\underline{U}_2\underline{G}_{2,0,\sigma}\\
&\qquad\qquad+\underline{U}_4\underline{G}_{4,0,\sigma}\ ,\\
&(\underline{1}E-\underline{V}_\beta^\sigma)\underline{G}_{2,0,\sigma}=\underline{V}_2\underline{G}_{1,0,\sigma}+\underline{V}_3\underline{G}_{7,0,\sigma}+\underline{V}_4\underline{G}_{9,0,\sigma}\ ,\\
&(\underline{1}E-\underline{V}_b-\underline{U}_1\underline{T}_1)\underline{G}_{7,0,\sigma}=\underline{V}_3\underline{G}_{2,0,\sigma}+\underline{V}_2\underline{G}_{6,0,\sigma}\\
&\qquad\qquad+\underline{V}_4\underline{G}_{8,0,\sigma}\ ,\\
&(\underline{1}E-\underline{V}_\alpha^\sigma)\underline{G}_{6,0,\sigma}=\underline{V}_2\underline{G}_{7,0,\sigma}+\underline{V}_3\underline{G}_{11,0,\sigma}+\underline{V}_4\underline{G}_{13,0,\sigma}\ ,\\
&(\underline{1}E-\underline{V}_b-\underline{V}_1\underline{T}_1)\underline{G}_{11,0,\sigma}=\underline{V}_3\underline{G}_{6,0,\sigma}+\underline{V}_2\underline{G}_{10,0,\sigma}\\
&\qquad\qquad+\underline{V}_4\underline{G}_{12,0,\sigma}\ ,
\end{aligned} \tag{8}$$

where $\underline{1}$ is the unit matrix, and

$$\underline{V}_\alpha^\sigma \equiv \begin{bmatrix} E_{\alpha,\sigma} & t_0 & t_0 & t_0 \\ t_0 & E_s & t_0 & t_0 \\ t_0 & t_0 & E_s & t_0 \\ t_0 & t_0 & t_0 & E_s \end{bmatrix},$$

$$\underline{V}_\beta^\sigma \equiv \begin{bmatrix} E_{\beta,\sigma} & t_0 & t_0 & t_0 \\ t_0 & E_s & t_0 & t_0 \\ t_0 & t_0 & E_s & t_0 \\ t_0 & t_0 & t_0 & E_s \end{bmatrix},$$

$$\underline{V}_b \equiv \begin{bmatrix} E_b & t_0 & t_0 & t_0 \\ t_0 & E_b & t_0 & t_0 \\ t_0 & t_0 & E_b & t_0 \\ t_0 & t_0 & t_0 & E_b \end{bmatrix},$$

$\underline{V}_1$ is a 4×4 matrix defining the interaction between the orbitals of nearest-neighbor atoms in the bulk, while $\underline{V}_2$, $\underline{V}_3$, and $\underline{V}_4$ define the interaction between the orbitals of the atoms of the first and second layers[23] (see Fig. 1). $\underline{G}_{n,0,\sigma}$ is a 4×4 matrix with elements $\underline{G}_{n0,ij,\sigma}$, where i and j run from 1 to 4, according to the orbitals of the atoms n and o. Finally, $\underline{T}_1$ is the transfer matrix for the bulk crystal.[23] Equation (8) can be solved by introducing the following transfer matrices:

$$T_s^{\text{in},\sigma}=G_{j'0,\sigma}(G_{j0,\sigma})^{-1},\quad T_s^{\text{out},\sigma}=G_{j0,\sigma}(G_{j'0,\sigma})^{-1},$$
$$\text{for } j' \text{ odd and } j \text{ even}. \quad (9)$$

In these equations s runs from 2 to 4 and depends on the direction of the bonds joining atoms j and j' (1 refers to the dangling bond orbital). Introducing Eq. (9) into Eqs. (8) we get the following equations:

$$\begin{aligned}
&(E\underline{1}-\underline{V}_b-\underline{V}_1\underline{T}_1-\underline{V}_2\underline{T}_2^{\text{out},\sigma}-\underline{V}_4\underline{T}_4^{\text{out},\sigma})\underline{V}_3=\underline{T}_3^{\text{in},\sigma},\\
&(E\underline{1}-\underline{V}_b-\underline{V}_1\underline{T}_1-\underline{V}_3\underline{T}_3^{\text{out},\sigma}-\underline{V}_4\underline{T}_4^{\text{out},\sigma})\underline{V}_2=\underline{T}_2^{\text{in},\sigma},\\
&(E\underline{1}-\underline{V}_\alpha^\sigma-\underline{V}_2\underline{T}_2^{\text{in},\sigma}-\underline{V}_4\underline{T}_4^{\text{out},\sigma})\underline{V}_3=\underline{T}_3^{\text{out},\sigma},\\
&(E\underline{1}-\underline{V}_\alpha^\sigma-\underline{V}_3\underline{T}_3^{\text{in},\sigma}-\underline{V}_4\underline{T}_4^{\text{in},\sigma})\underline{V}_2=\underline{T}_2^{\text{out},\sigma},
\end{aligned} \quad (10)$$

for the transfer matrices $\underline{T}_2^{\text{in},\sigma}$, $\underline{T}_2^{\text{out},\sigma}$, $\underline{T}_3^{\text{in},\sigma}$, and $\underline{T}_3^{\text{out},\sigma}$. [Note that $\underline{T}_4^{\text{out},\sigma}$ and $\underline{T}_4^{\text{in},\sigma}$ are related to $\underline{T}_2^{\text{out},\sigma}$ and $\underline{T}_2^{\text{in},\sigma}$ through a mirror plane symmetry of the (2×1) surface.]

Equations (10) yield the different transfer matrices and allow us to calculate $\underline{G}_{00,\sigma}$ [see Eqs. (8)]:

$$\underline{G}_{00,\sigma}=(\underline{E}-\underline{V}_\alpha^\sigma-\underline{V}_3\underline{T}_3^{\text{in},\sigma}-\underline{V}_2\underline{T}_2^{\text{in},\sigma}-\underline{V}_4\underline{T}_4^{\text{in},\sigma})^{-1}. \quad (11)$$

From this equation we can obtain the density of states associated with the orbitals of the surface layer:

$$n_{d,\sigma}^\alpha(u)=-\frac{1}{\pi}\text{Im}G_{00,11,\sigma}(\omega), \quad (12a)$$

$$n_{d,\bar\sigma}^\beta(\omega)=-\frac{1}{\pi}\text{Im}G_{00,11,\sigma}(\omega), \quad (12b)$$

$$n_{s,\sigma}^\alpha(\omega)=-\frac{1}{\pi}\text{Im}G_{00,22,\sigma}(\omega), \quad (12c)$$

and

$$n_{s,\bar\sigma}^\beta(\omega)=-\frac{1}{\pi}\text{Im}G_{00,22,\sigma}(\omega). \quad (12d)$$

B. Results

The parameters of Hamiltonian (1) have been taken from Ref. 23. The s and p levels of Si are taken as follows:

$$E_p-E_s=8 \text{ eV}, \quad (13)$$

while the hopping integrals are defined by the following interactions:

(i) $ss\sigma$—first neighbors interaction: -1.65 eV;
(ii) $ss\sigma$—first neighbors interaction: -2.16 eV;
(iii) $pp\sigma$—first neighbors interaction: 3.35 eV;
(iv) $pp\pi$—first neighbors interaction: -1.00 eV,

which were adjusted to give an appropriate density of states for the bulk bands calculated with the Bethe-lattice method.

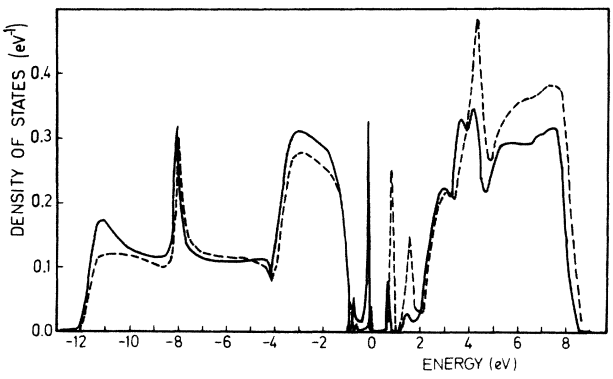

FIG. 3. Local density of states for the surface layer of the Si(111)-(2×1) face, with $U=5.5$ eV. Solid line: spin up. Dashed line: spin down.

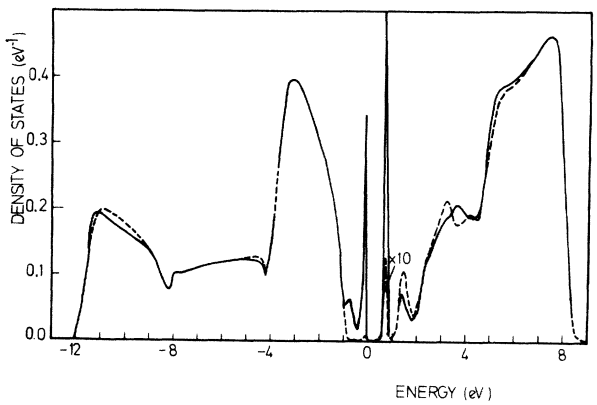

FIG. 4. Local density of states for the first sublayer of the Si(111)-(2×1) face, with $U=5.5$ eV. Solid line: spin up. Dashed line: spin down.

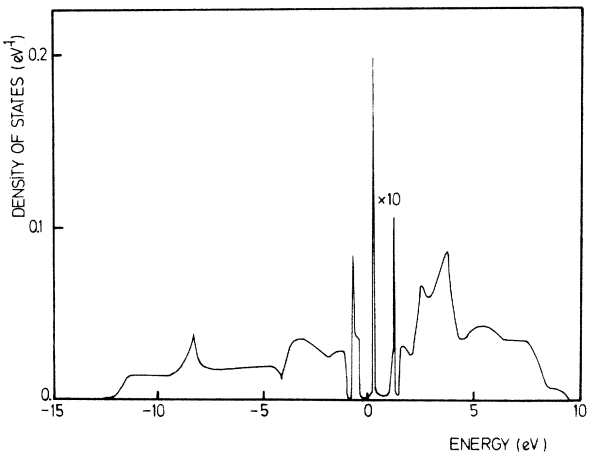

FIG. 5. Local density of states for the dangling bond of the paramagnetic Si(111)-(1×1) face, with $U=6$ eV.

As regards the intrasite Coulomb interaction, we follow Ref. 22 and take $U=5.5$ eV. As discussed in Ref. 22, this value is equivalent to the effective value of 1.5 eV taken for the two-dimensional models of the surface states.

In Figs. 2, 3, and 4 we present our results for the electronic density of states on the dangling bond, the surface layer, and the first sublayer for spins up and down of the (2×1) surface. In Fig. 5 we present the density of states for the paramagnetic state of Si(111)-1×1, for comparison. In the Si(111)-(2×1) surface we find that the surface bands present *four* different peaks. Two peaks, located roughly at $E_F\pm0.8$ eV, are similar to the ones found in the Si(111)-(1×1) face, while the two other peaks defining the fundamental energy gap (~0.6 eV) can be understood as coming from the splitting of the Kondo-like peak that appears for the Si(111)-(1×1) face. The weights of the four peaks for the (2×1) face differ, however, from the weights found in the (1×1) surface; thus in the (2×1) surface each peak at $E_F\pm1.0$ eV has a weight of about 0.21, while the weight of each of the two central peaks are close to 0.29; the reason is that in the present calculation the peak at $E_F-0.8$ eV (or $E_F+0.8$ eV) is rather close to the other peak coming from the Kondo-like peak splitting. Regardless, our results show that correlation effects are very important for both the paramagnetic and the antiferromagnetic states, and that the density of states found for $U=5.5$ eV is close to the one calculated in a two-dimensional model by taking an effective value close to 1.5 eV for the intrasite Coulomb interaction.[18]

IV. ELECTRON-PHONON EFFECTS

A. Method of calculation

Let us now concentrate in solving the Hamiltonian (2), where $\hat{N}_s$ is the occupation number operator of the electrons filling the surface-state bands (we shall neglect temperature effects that in this case are not expected to be important). Consider, in a first step, the paramagnetic solution.[22] As Fig. 5 shows, surface states present three peaks in the density of states: At the Fermi level there appears a Kondo-like resonance, and at $E_F\pm0.8$ eV we find two other broader bands. Since 0.8 eV is much greater than the phonon frequency ($\omega_0\sim0.062$ eV), we propose to analyze the electron-phonon coupling by considering each peak separately and by using the renormalization arguments applied to quasiparticles.[24]

Consider, for simplicity, the band located at $E\simeq E_F-0.8$ eV. This band is associated with the creation of a high energetic hole; this hole corresponds to the creation of a strong fluctuation of charge ($\Delta n\simeq1$) at the surface atom and. for this case, we expect to have *no* renormalization in the electron-phonon coupling of the quasiparticle. The effect of the electron-phonon coupling in the electron density of states for this peak can be analyzed by means of an appropriate diagonal self-energy, $\Sigma^i_{e\text{-ph}}(\omega)$. Similar to the analysis of electron correlation effects, we calculate that local self-energy to all orders of the coupling by means of an interpolation scheme (although details will be published elsewhere,[25] we give here a brief summary of the procedure). In our method, we obtain the electron-phonon coupling in two limits: $g\to0$ and $W\to0$ (W is the width of the peak). For $g\to0$, the lowest perturbation approach is adequate and yields

$$\Sigma^{(1)s}_{e\text{-ph}}=g\omega_0^2\int\frac{n_s(E')}{\omega+\omega_0-E'}dE' , \tag{14}$$

where $n_s(E)$ is the density of states associated with the peak we are considering. For $W\to0$, the self-energy can be obtained from the exact Green function given in Ref. 26:

$$G(\omega)=\frac{1}{\omega-\Sigma^s_{e\text{-ph}}(\omega)}=e^{-g}\sum_{l=0}^{\infty}\frac{g^l/l!}{\omega+\omega_0(g-1)} . \tag{15}$$

(Energies are referred to the center of the peak.) Since we are interested in an intermediate case, we look for an interpolation between these two limits following the argument given in Ref. 27. Thus, by taking the limit $W\to0$ in Eq. (14) [or $g\to0$ in Eq. (15)], one has

$$\lim_{W\to0}\Sigma^{(1)s}_{e\text{-ph}}(\omega)=\frac{g\omega_0^2}{\omega-\omega_0} . \tag{16}$$

Now, we define the following equations:

$$\Sigma^{(1)s}_{e\text{-ph}}=\frac{g\omega_0^2}{\Omega-\omega_0} , \tag{17a}$$

$$\frac{1}{\Omega-\Sigma^s_{e\text{-ph}}(\omega)}=e^{-g}\sum_{g=0}^{\infty}\frac{g^l/l!}{\Omega+\omega_0(g-l)} . \tag{17b}$$

By eliminating Ω between Eqs. (17a) and (17b), we obtain a relationship between $\Sigma^s_{e\text{-ph}}(\omega)$ and $\Sigma^{(1)s}_{e\text{-ph}}$ [this last self-energy being defined by Eq. (4)]. This relationship gives the interpolated expression we are looking for; indeed, it is easy to show that the defined self-energy, $\Sigma^s_{e\text{-ph}}(\omega)$, yields the appropriate limits for $g\to0$ and $W\to0$.

For the Kondo-like peak, things are slightly different since we have for this case excitations of very low energy, associated with a smaller fluctuation of electronic charge at each atom.[25] The quasiparticle renormalization method[24] shows that the electron-phonon coupling for the

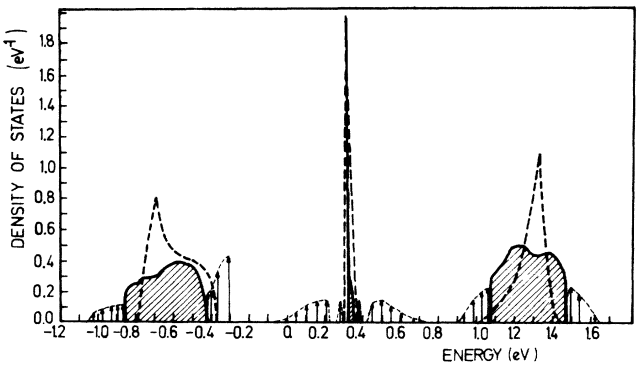

FIG. 6. Local density of states around E_F for the paramagnetic state of the Si(111)-(1×1) face. Dashed line: only correlation effects included. Solid line: electron-phonon coupling included.

Kondo-like peak has to decrease, as compared with the previous case, by a factor proportional to the square root of the corresponding weight for the quasiparticle. This suggests substitution of approximately (for the Kondo-like peak) $g^{1/2}$ for $(g/3)^{1/2}$ (we have taken an effective g coupling of 1.2 for this peak and 3.6 for the other peaks).

Let us now turn our attention to the antiferromagnetic Si(111)-(2×1) face. The electronic density of states drawn in Figs. 2 and 3 shows that for this face we have two filled (or empty) peaks per spin associated with the surface states, which are rather close in energy and have similar weights. We have analyzed the electron-phonon coupling effects on this density of states by following the argument given above: Since the two peaks previously mentioned are very close and their separation is reduced by the electron-phonon coupling, we have introduced a local self-energy $\Sigma^s_{e\text{-ph}}(\omega)$ as a function of the local density of states in the dangling bond by considering *simultaneously* the two peaks per spin calculated in the preceding section, without any g renormalization (in similarity with the treatment given in the paramagnetic state to the peak found below the Fermi level). This means that Eqs. (17a) and (17b) define $\Sigma^s_{e\text{-ph}}(\omega)$ as a function of $\Sigma^{(1)s}_{e\text{-ph}}(\omega)$, with this self-energy given by Eq. (14), $n_s(E)$ being the density of surface states shown in Fig. 2.

B. Results

Figures 6 and 7 show the local density of electronic surface states for the two cases of Si(111)-(1×1) and -(2×1) faces. Figure 7 shows the total density of states for the (2×1) face, including spins up and down. Comparing with Figs. 2 and 3, we see that the main effects of the electron-phonon coupling are threefold: (i) first, we see that there is an important broadening of the electronic states—the final states are around 50% wider than the initial density of states; (ii) on the other hand, the two peaks below (or above) the Fermi level are strongly overlapping; (iii) finally, the energy gap between the two density of states for spins up and down is partially filled by the satellite structure introduced by the electron-phonon coupling. Note that the final gap has been reduced from 0.6 to 0.25 eV.

In Fig. 6 we show the total density of surface states for the paramagnetic (1×1) surface. In this case, we find results similar to the ones reported for a two-dimensional model.[16] Again, the two peaks around $E_F \pm 0.8$ eV are strongly broadened by the electron-phonon coupling. At the same time, the Kondo-like peak is narrowed, and a new satellite structure appears at $E_F \pm 0.2$ eV. The final width of the Kondo-like peak is 20 meV; for this case, temperature effects[16] would tend to eliminate all the structure shown in Fig. 6 around the Fermi level. At room temperature, we expect that only the peaks at $E_F - 0.8$ eV and $E_F - 0.20$ eV could be observed. At this point, it could be of interest to remark that according to the calculation of Ref. 28, for the ideal Si(111) surface, the antiferromagnetic state is more stable than the paramagnetic one.

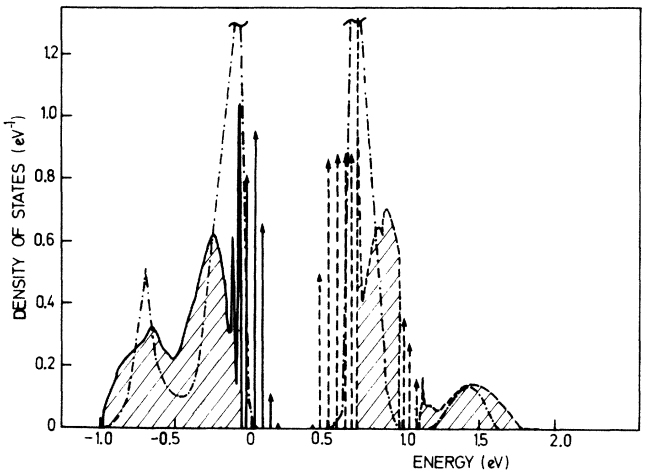

FIG. 7. Local density of states around E_F for the antiferromagnetic Si(111)-(2×1) face. Solid line: only correlation effects included for spin up. Dashed line: only correlation effects included for spin down. Dashed-dotted line: electron-phonon coupling included for spin up and spin down.

V. CONCLUDING REMARKS

In this paper we have calculated the electron density of surface states for the paramagnetic and antiferromagnetic Si(111) face. In our calculation, many-body effects associated with electron correlation and electron-phonon coupling are included. Our results have been performed by using a Bethe-lattice approximation for the crystal electronic structure, and by using Green-function techniques and appropriate self-energies that include electron-electron and electron-phonon effects. Our final results for the electronic density of surface states show a remarkable agreement with independent results calculated by using two-dimensional models.[17,18] In particular, the paramagnetic phase shows a very narrow Kondo-like peak at the Fermi level, two satellites at $E_F \pm 0.2$ eV, and two broader peaks at $E_F \pm 0.8$ eV. The antiferromagnetic (2×1) phase shows four different peaks, two of them located at $E_F \pm 0.8$ eV and two other at $E_F \pm 0.4$ eV; the energy gap due to correlative effects, which is around 0.6 eV, is reduced by electron-phonon coupling to a final value of 0.25 eV.

In conclusion, our calculation shows the great importance that correlation and electron-phonon coupling effects have on the electronic properties of the surface states of Si(111).

[1]D. Zehner, C. W. White, P. Heimann, B. Reihl, F. J. Himpsel, and D. E. Eastman, Phys. Rev. B **24**, 4875 (1981).
[2]Y. J. Chabal, J. E. Rowe, and D. A. Zwemer, Phys. Rev. Lett. **46**, 600 (1981).
[3]K. C. Pandey, Phys. Rev. Lett. **47**, 1913 (1981).
[4]R. M. Tromp, L. Smit, and J. F. van der Veen, Phys. Rev. B **30**, 6235 (1984).
[5]M. A. Olmstead and N. H. Amer, Phys. Rev. Lett. **52**, 1148 (1984).
[6]P. Chiaradia, A. Cricenti, S. Selci, and G. Chiarotti, Phys. Rev. Lett. **52**, 1145 (1984).
[7]H. Liu, M. Cook, F. Jona, and P. M. Marcus, Phys. Rev. B **28**, 6137 (1983).
[8]F. J. Himpsel, P. Heinemann, and D. E. Eastman, Phys. Rev. B **24**, 2003 (1981).
[9]R. F. G. Uhrberg, G. V. Honsson, J. M. Nicholls, and S. A. Flodström, Phys. Rev. Lett. **48**, 1032 (1982).
[10]J. E. Northrup and M. L. Cohen, Phys. Rev. Lett. **49**, 1349 (1982).
[11]F. J. Himpsel, Phys. Rev. B **27**, 7782 (1983).
[12]E. G. McRae, Phys. Rev. B **28**, 2305 (1983).
[13]G. Binnig, H. Rohrer, Ch. Gerber, and E. Weibel, Phys. Rev. Lett. **50**, 120 (1983).
[14]J. E. Demuth, B. N. J. Persson, and A. J. Sorokin, Phys. Rev. Lett., **51**, 2214 (1983).
[15]S. Yokotsuka, S. Kono, S. Susuki, and T. Sagawa, Solid State Commun. **46**, 401 (1983).
[16]F. Flores, C. Tejedor and E. Louis, in *Proceedings of the 17th International Conference on the Physics of Semiconductors,* edited by J. D. Chadi and W. A. Harrison (Springer, Berlin, 1985), p. 47.
[17]E. Louis, F. Flores, F. Guinea, and C. Tejedor, Solid State Commun. **44**, 1633 (1982).
[18]A. Martín-Rodero, E. Louis, F. Flores, and C. Tejedor, Phys. Rev. B **29**, 476 (1984).
[19]D. Weare and M. F. Thorpe, Phys. Rev. B **4**, 2508 (1971).
[20]F. Guinea and C. Tejedor, J. Phys. C **13**, 5515 (1980); C. Strinati, H. J. Mattausch, and W. Hanke, *ibid.* **25**, 2867 (1982); C. S. Wang and W. E. Pickett, Phys. Rev. Lett. **51**, 597 (1983).
[21]J. Sánchez-Dehesa, F. Guinea, and C. Tejedor, J. Phys. C **14**, 3355 (1981).
[22]A. Muñoz, F. Flores, C. Tejedor, and E. Louis, Surf. Sci. **152—153**, 1027 (1985).
[23]E. Louis and F. Ynduráin, Phys. Rev. B **16**, 1542 (1977).
[24]P. Nozières, *Theory of Interacting Fermi Systems* (Benjamin, New York, 1964).
[25]C. Tejedor, F. Flores, and E. Louis, J. Phys. C (to be published).
[26]G. D. Mahan, *Many-Particle Physics* (Plenum, New York, 1981).
[27]A. Martín-Rodero, M. Baldo, F. Flores, and R. Pucci, Solid State Commun. **44**, 911 (1982).
[28]J. E. Northrup and M. L. Cohen, Phys. Rev. B **29**, 5944 (1984).